

Modeling and Analysis of Active Flutter Suppression of the Prepositive Elliptical Wing-Main Wing Composite Configuration

Congyu Zhao[1,2], Baigang Mi[1,2], Xuan Bai[1,2]

[1] Northwestern Polytechnical University, School of Aeronautics, Xi'an, 710072, China;
[2] National Key Laboratory of Aircraft Configuration Design, Xi'an, 710072, China.

Abstract

Flutter is a self-excited aeroelastic instability caused by the coupling among aerodynamic, inertial, and elastic forces. Conventional active flutter suppression methods usually rely on control-surface deflection to modify the aerodynamic damping of the system, but they may introduce additional drag, aerodynamic efficiency loss, and load coupling. To reduce the dependence on conventional main-wing control surfaces, this paper investigates the flutter response characteristics of a two-dimensional prepositive elliptical wing–main wing combined configuration. In this configuration, a prepositive elliptical wing is installed upstream of the main wing and acts as a relatively independent aerodynamic interference component. Its flow circulation, induced flow, and wake disturbance modify the unsteady aerodynamic loads and aerodynamic energy input acting on the main wing.

A time-domain computational fluid dynamics method is established to simulate the free aeroelastic response of a NACA0012 main wing with plunge and pitch degrees of freedom. An overset-grid method is used to handle the pre-wing–main wing combined configuration, and a user-defined function is adopted to couple the unsteady aerodynamic loads with the two-degree-of-freedom structural dynamic equations. A baseline main-wing case at $U_\infty = 55\mathrm{m/s}$ is first calculated and used as the reference for the subsequent combined configurations. The effects of the pre-wing position and size on the aeroelastic response of the main wing are then analyzed in terms of structural response amplitude, nondimensional aerodynamic work, and the time evolution of aerodynamic forces and structural velocities.

The results show that the pre-wing position has a significant influence on the coupled plunge–pitch response of the main wing. Within the investigated design space, most combined configurations reduce both the plunge and pitch amplitude. Relatively favorable positions are mainly located around $\bar{L}_H = 0.08 \sim 0.10$ and $\bar{L}_V = 0.04 \sim 0.06$, where the maximum reductions of both plunge and pitch amplitudes reach approximately 85%. The aerodynamic-work analysis indicates that the reduction in the plunge-channel aerodynamic work is the main reason for the suppressed aeroelastic response of the main wing. For the representative favorable positions (0.08,0.04) and (0.10,0.06), the plunge-channel aerodynamic work is reduced by approximately 98%.

Meanwhile, some special positions show large reductions in total aerodynamic work while the structural response amplitudes increase. This indicates that total aerodynamic work alone is insufficient for evaluating the flutter suppression effect of the pre-wing, and that channel-wise aerodynamic work should be considered together with structural response amplitudes. The time-evolution analysis of aerodynamic forces and structural velocities shows that the relatively stationary pre-wing does not significantly change the dominant phase relationship. Its main effect is reflected in the modification of aerodynamic-force amplitudes and the redistribution of aerodynamic energy between the plunge and pitch channels.

The preliminary size analysis further shows that reducing the major-axis length of the pre-wing weakens its ability to suppress the aeroelastic response of the main wing. These results provide a preliminary CFD-based analysis of the mechanism by which the prepositive elliptical wing–main wing combined configuration

https://doi.org/10.71945/icas2026_0494

influences flutter response.

Keywords: Aeroelastic response; Aerodynamic work; Overset grid; Prepositive elliptical wing

1. Introduction

Flutter is an aeroelastic instability phenomenon caused by the coupling among aerodynamic, elastic and inertial forces. When the energy input from unsteady aerodynamic loads cannot be sufficiently dissipated by structural damping, a lifting surface may develop divergent oscillations once the flight speed exceeds the critical flutter speed. This phenomenon may lead to severe structural damage or catastrophic failure and has therefore remained one of the key safety issues in aircraft design [1,2]. With the development of lightweight structures, high-aspect-ratio wings, flexible lifting surfaces, and unconventional aircraft configurations, the interaction between structural deformation and unsteady aerodynamics becomes increasingly significant. As a result, accurate flutter prediction and effective flutter suppression are crucial for enhancing flight safety, expanding the flight envelope, and mitigating design risk for new aircraft configurations [3].

Accurate modeling of unsteady aerodynamic loads provides the foundation for flutter analysis and flutter suppression design. Wagner proposed a classical time-domain description of the dynamic lift build-up process, while Theodorsen established a frequency-domain theory for oscillating airfoils and airfoil–aileron systems, which has become one of the fundamental tools for linear flutter analysis [1,4]. For large-angle-of-attack or stall-related aeroelastic problems, nonlinear aerodynamic models have been developed to account for aerodynamic hysteresis and flow-memory effects. The ONERA dynamic-stall model has been used to represent nonlinear stall aerodynamics, while the Leishman–Beddoes model provides a semi-empirical framework for describing dynamic stall and vortex-induced aerodynamic loads [5,6]. Goman and Khrabrov proposed a state-space representation of aerodynamic characteristics at high angles of attack by introducing internal variables associated with flow separation [7]. In addition, computational fluid dynamics/computational structural dynamics coupling and reduced-order modeling have been increasingly adopted to retain high-fidelity unsteady aerodynamic information at an acceptable computational cost. Tang and Dowell established aeroelastic models for high-aspect-ratio wings and conducted wind tunnel tests to study flutter and limit-cycle oscillations [8]. Skujins and Cesnik developed reduced-order models for unsteady aerodynamics across different Mach-number regimes and showed that such models can reproduce the main features of high-fidelity CFD results with significantly improved efficiency [9].

Active flutter suppression has been extensively investigated as an effective approach to increasing the flutter boundary and suppressing unstable aeroelastic responses. Nissim introduced an active control method based on the aerodynamic-energy concept, in which control surfaces are used to change the work done by aerodynamic forces on the elastic structure [10]. This idea provided an early physical interpretation of flutter suppression from the viewpoint of energy exchange between the flow field and the structure. With the development of modern control theory, many studies have focused on applying optimal, robust, adaptive, and intelligent control methods to aeroelastic systems. For two-dimensional airfoil sections with plunge, pitch, and control-surface degrees of freedom, linear quadratic regulator and linear quadratic Gaussian controllers have been widely used to increase effective aerodynamic damping and suppress limit-cycle oscillations. Behal et al. designed an output-feedback adaptive control law for a nonlinear two-dimensional lifting surface, in which the pitch angle was driven toward a prescribed nominal value and the influence of model-parameter uncertainty was compensated adaptively [11]. Their results showed that the closed-loop system could achieve asymptotic stability and reduce vibration energy in the subcritical velocity range. Na et al. developed a robust estimation methodology for flapped wing systems, using observer-based control to improve state estimation and enhance the effectiveness of the controller [12].

Robust control strategies have also been widely studied for flutter suppression under parameter uncertainty and external disturbances. Yu et al. designed an H_∞controller for a two-dimensional airfoil section with a control surface, considering uncertainties in plunge damping, pitch damping, and actuator parameters [13]. They further developed a μ-synthesis controller and showed that it provided improved robustness compared with the conventional H_∞design [14]. Hou et al. proposed

a robust adaptive switching control method based on multiple Lyapunov functions and model-reference adaptive control theory [15]. By switching among controllers designed for different velocity points, the method avoided the restriction that adaptive parameters must vary slowly and improved the flutter suppression performance over a wider velocity range. Si and Zhao developed a flutter suppression method based on an LQG self-tuning regulator [16]. A variable forgetting-factor algorithm was used for real-time parameter identification, a Kalman filter was adopted for state reconstruction, and the control law was obtained by solving the discrete-time algebraic Riccati equation. Their results demonstrated that this method could effectively suppress flutter and maintain a certain degree of robustness.

In addition to classical control-surface-based methods, researchers have also explored active materials, smart structures, and flow-control-based approaches for aeroelastic stabilization. Han et al. investigated active flutter suppression of a lifting surface using piezoelectric actuation and modern control theory, showing that piezoelectric actuators can provide additional control authority without relying solely on traditional aerodynamic control surfaces [17]. Other studies have introduced morphing structures or leading-edge and trailing-edge control mechanisms to improve control efficiency and reduce required deflection amplitudes. Active flow control methods, such as leading-edge blowing, synthetic jets, plasma actuation, and circulation control, have been used to modify separated flow structures and reduce unsteady aerodynamic loads. Chen et al. experimentally investigated stall flutter suppression of a NACA0012 airfoil using steady leading-edge blowing [18]. Their results showed that leading-edge blowing can suppress the formation and shedding of dynamic stall vortices, reduce aerodynamic moment fluctuations, shrink aerodynamic hysteresis loops, and promote the decay of self-excited oscillations. These studies indicate that active modification of the local flow field can influence the aerodynamic energy transferred to the structure and therefore has potential for flutter suppression.

Although the above active flutter suppression methods have achieved significant progress, several practical limitations remain. Conventional control-surface deflection may introduce additional drag, aerodynamic efficiency degradation, and load coupling. Actuator bandwidth, saturation, free play, model uncertainty, and control-loop delay can further reduce the achievable suppression performance. Meanwhile, emerging actuation concepts such as piezoelectric actuation, morphing structures, and jet-based flow control may involve challenges related to actuation authority, energy consumption, structural integration, reliability, and airworthiness verification [3,17,18]. These limitations motivate the exploration of new configurations that can modify aerodynamic energy input while reducing dependence on conventional main-wing control-surface deflection.

Motivated by these considerations, this study investigates a prepositive elliptical wing–main wing combined configuration. In this configuration, a small prepositive elliptical wing, hereafter referred to as the pre-wing, is installed upstream of the main wing. Instead of directly deflecting the main-wing control surface, the pre-wing modifies the incoming flow condition, wake disturbance, and aerodynamic energy input acting on the main wing. Previous studies on the prepositive elliptical wing–main wing combined configuration have shown that the pre-wing can regulate the flow near the leading edge of the main wing and improve the anti-separation capability of the boundary layer at high angles of attack [19,20]. Bai et al. established an unsteady aerodynamic force modeling method for this configuration by introducing the geometric and dynamic motion parameters of the pre-wing into a physically interpretable state-space model [20]. Their results demonstrated that the pre-wing can significantly affect the unsteady aerodynamic behavior of the combined system and that the aerodynamic characteristics are strongly related to the pre-wing size, position, and motion parameters.

The flow-control mechanism of the prepositive elliptical wing–main wing combined configuration is closely related to the interaction between the pre-wing wake and the main-wing leading-edge flow. The gap between the pre-wing and the main wing can produce a channel effect similar to that of a leading-edge slat, accelerating the flow toward the upper surface of the main wing and increasing the local boundary-layer energy. Meanwhile, the wake generated by the pre-wing can alter the phase characteristics of the unsteady aerodynamic loads on the main wing. From the perspective of aeroelastic energy, this phase change may influence the aerodynamic work over one oscillation

https://doi.org/10.71945/icas2026_0494

cycle and modify the equivalent aerodynamic damping of the system. Previous CFD results have shown that, for a NACA0012 main wing, a stationary pre-wing can increase the lift-to-drag ratio from 4.1475 to 17.4144, corresponding to a maximum improvement of approximately 319% [19]. A small-amplitude vibrating pre-wing can further enhance the wake energy, leading to a maximum lift-to-drag ratio improvement of approximately 485% [19]. In the small-angle-of-attack range of 0°–12°, the pre-wing does not produce significant adverse effects on the original lift-to-drag performance of the main wing and may even provide a slight improvement [19].

In this work, the flutter characteristics of a two-dimensional prepositive elliptical wing–main wing combined configuration are investigated using time-domain computational fluid dynamics simulations. The free aeroelastic responses of a baseline main wing and the combined configuration are compared under representative flow conditions. The unsteady aerodynamic loads, plunge response, pitch response, aerodynamic work, and phase relationship between aerodynamic forces and structural motion are extracted to clarify the aerodynamic-energy mechanism of the configuration. The effects of different pre-wing positions on the flutter response, aerodynamic work, and phase difference are then analyzed. The objective of this study is to provide a preliminary CFD-based assessment of the flutter suppression characteristics of the combined configuration and to establish a basis for subsequent reduced-order aerodynamic modeling and active pre-wing phase-control design.

2. Aerodynamic characteristics and basic principle of the prepositive elliptical wing–main wing combined configuration

2.1 Aerodynamic characteristics under flutter conditions

Flutter is a typical aeroelastic dynamic instability. It is essentially a self-excited vibration caused by the coupling among structural elastic motion, inertial forces, and unsteady aerodynamic forces. For a two-dimensional airfoil system, when the main wing undergoes plunge and pitch motions in the incoming flow, its instantaneous effective angle of attack and surface pressure distribution vary with time, resulting in unsteady lift and pitching moment. These unsteady aerodynamic forces then act back on the structural system and further modify the motion of the main wing. When the aerodynamic forces input more energy into the structure over one oscillation cycle than the energy dissipated by structural damping, the vibration amplitude increases gradually. When the incoming flow velocity reaches a critical value, the system changes from decaying oscillation to constant-amplitude or divergent oscillation. This critical state is referred to as the flutter boundary.

Under the linear small-disturbance assumption, the classical flutter problem of a two-dimensional airfoil section is commonly described using Theodorsen's unsteady aerodynamic theory. This theory is based on incompressible, inviscid, thin-airfoil assumptions with small-amplitude harmonic motion. The unsteady aerodynamic forces acting on an oscillating airfoil are divided into non-circulatory and circulatory components. The non-circulatory aerodynamic force mainly originates from the fluid added-mass effect and is related to the acceleration of the airfoil motion. The circulatory aerodynamic force is associated with circulation variation, wake-vorticity convection, and aerodynamic lag induced by the wake. The Theodorsen function $C(k)$ is used to describe the amplitude attenuation and phase lag of the circulatory aerodynamic force with reduced frequency, and can be written as

$$C(k) = F(k) + iG(k) \tag{1}$$

where $k = \dfrac{\omega b}{U_\infty}$ is the reduced frequency, b is the airfoil semi-chord, ω is the oscillation circular frequency, and U_∞ is the freestream velocity. This function indicates that the unsteady aerodynamic forces acting on an oscillating airfoil depend not only on the instantaneous effective angle of attack, but also on the structural motion frequency, wake development, and aerodynamic phase lag.

In two-dimensional thin-airfoil theory with small disturbances, Theodorsen's aerodynamic force can be expressed in a simplified form as

$$L_c = 2\pi\rho U_\infty^2 b C(k)\alpha_{\text{eff}} \tag{2}$$

where L_{nc} is the non-circulatory aerodynamic force related to motion acceleration, and L_c is the

https://doi.org/10.71945/icas2026_0494

circulatory aerodynamic force associated with circulation and wake effects. The circulatory lift can be written as

$$\alpha_{\text{eff}} = \alpha + \frac{\dot{h}}{U_\infty} + \left(\frac{1}{2} - a_e\right)\frac{b\dot{\alpha}}{U_\infty} \tag{3}$$

where a_e is the nondimensional elastic-axis position with respect to the semi-chord, and α_{eff} is the effective angle of attack determined by the pitch angle, plunge velocity, and pitch rate. This expression shows that the circulatory aerodynamic force contains both amplitude attenuation and phase lag through $C(k)$, and therefore reflects the influence of the wake on the unsteady aerodynamic force.

For a two-degree-of-freedom airfoil section with plunge and pitch motions, the generalized coordinate vector of the main wing can be defined as $\mathbf{q} = [h, \alpha]^T$, where h is the plunge displacement and α is the pitch angle. The corresponding aeroelastic governing equation can be written as

$$\mathbf{M}_s\ddot{\mathbf{q}} + \mathbf{C}_s\dot{\mathbf{q}} + \mathbf{K}_s\mathbf{q} = \mathbf{Q}_a \tag{4}$$

where $\mathbf{M}_s$, $\mathbf{C}_s$ and $\mathbf{K}_s$ are the structural mass, damping, and stiffness matrices, respectively, and $\mathbf{Q}_a$ is the generalized aerodynamic-force vector. In this study, the generalized aerodynamic forces are mainly composed of the lift-direction aerodynamic force $F_y(t)$ and the pitching moment about the elastic axis $M_z(t)$, namely $\mathbf{Q}_a = \left[F_y(t), M_z(t)\right]$.

From the energy perspective, the occurrence of flutter depends not only on the magnitude of aerodynamic forces but also on the phase relationship between the aerodynamic forces and structural velocities. Over one oscillation cycle, the aerodynamic work done on the structural system can be expressed as

$$W_a = \int \left[F_y(t)\dot{h}(t) + M_z(t)\dot{\alpha}(t)\right]dt \tag{5}$$

where $F_y(t)\dot{h}(t)$ represents the instantaneous aerodynamic power in the plunge channel, and $M_z(t)\dot{\alpha}(t)$ represents the instantaneous aerodynamic power in the pitch channel. When $W_a > 0$, the aerodynamic forces input net energy into the structure over one cycle, corresponding to negative aerodynamic damping, and the structural vibration tends to grow. When $W_a < 0$, the aerodynamic forces extract energy from the structure, corresponding to positive aerodynamic damping, and the structural response tends to decay. Therefore, the sign and magnitude of aerodynamic work can directly indicate whether the unsteady aerodynamic forces promote or suppress the flutter response. It should be noted that, in a coupled plunge–pitch system, the total aerodynamic work is jointly determined by the two degree-of-freedom channels. In some cases, the lift may do positive work on the plunge motion, while the pitching moment may do negative work on the pitch motion; the opposite situation may also occur. Therefore, analyzing only the total aerodynamic work may not accurately reveal the source of flutter-response variation. In the following analysis, the aerodynamic work is further decomposed into the plunge and pitch channels, and combined with structural response amplitudes and the time evolution of aerodynamic forces and structural velocities to investigate the mechanism by which the prepositive elliptical wing affects the flutter response of the main wing.

2.2 Basic principle of flutter control using the prepositive elliptical wing

The object of this study is the prepositive elliptical wing–main wing combined configuration, as shown in the Fig 1. In this configuration, a small elliptical wing component, hereafter referred to as the pre-wing, is installed near the leading edge of the main wing. The pre-wing is not rigidly connected to the main wing. Its main function is not to directly change the geometric shape of the main wing like a conventional control surface, but to modify the incoming-flow condition near the leading edge of the main wing through its own flow circulation, induced velocity, and wake disturbance. In this way, the pre-wing affects the surface pressure distribution and unsteady aerodynamic response of the main wing. Compared with conventional control-surface deflection, the

https://doi.org/10.71945/icas2026_0494

pre-wing can be arranged upstream of the main wing as a relatively independent aerodynamic interference component, and its motion state can conceptually be controlled by an independent actuator, thereby reducing the dependence on main-wing control-surface deflection.

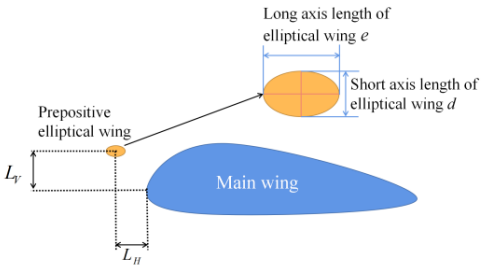


Figure 1 – Pre-main wing composite configuration

From the viewpoint of configuration composition, the prepositive elliptical wing–main wing combined configuration consists of two aerodynamic components: the main wing and the pre-wing. The main wing remains the primary lift-generating component, while the pre-wing acts as a flow-regulation component near the leading edge. The size, installation position, initial angle of attack, and motion state of the pre-wing can all change the way it interferes with the incoming flow of the main wing. When the pre-wing remains stationary relative to the main wing, it mainly modifies the local flow near the leading edge of the main wing and the wake-interference intensity through its fixed geometric arrangement. When it undergoes small-amplitude active oscillation, the pre-wing can generate a periodic wake disturbance, further changing the unsteady aerodynamic force input to the main wing (Fig 2).

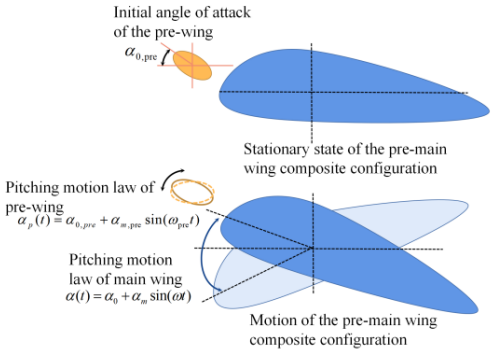


Figure 2 – Comparison between stationary and oscillating pre-wing states

The flutter-control problem investigated in this study is mainly associated with classical coupled plunge–pitch flutter under low-speed, incompressible, and small-disturbance conditions. Unlike dynamic-stall flutter at high angles of attack, classical flutter generally does not rely on large-scale flow separation. Its essence is the energy coupling between the plunge–pitch motion of the main wing and the unsteady aerodynamic forces. When aerodynamic forces continuously input energy into the structure over one oscillation cycle, the equivalent damping of the system decreases, and the structural response may change from decaying oscillation to constant-amplitude or divergent oscillation. Therefore, if the pre-wing can modify the magnitude, phase relationship, or energy-input path of the unsteady aerodynamic forces near the main wing, the flutter response may be weakened.

The prepositive elliptical wing–main wing combined configuration originally arises from the concept of flow control. Previous flow-control studies have shown that the pre-wing can regulate the flow structure near the leading edge of the main wing, improve the anti-separation capability of the boundary layer, and enhance the aerodynamic performance of the main wing under certain conditions. Although this paper focuses on low-speed classical flutter rather than high-angle-of-attack separation control, the two problems share a related physical mechanism: in both cases, the pre-wing modifies the local flow state near the leading edge of the main wing and thereby affects the surface pressure distribution and unsteady aerodynamic forces of the main wing.

In the classical flutter problem, the influence of the pre-wing on the main wing can be understood

https://doi.org/10.71945/icas2026_0494

from the perspective of aerodynamic energy. When the pre-wing is arranged upstream of the main wing, its local induced velocity, wake disturbance, and the channel effect between the pre-wing and the main wing can modify the instantaneous effective incoming-flow condition of the main wing. As a result, the lift and pitching moment of the main wing change compared with the baseline single-wing configuration. If such changes reduce the positive-work contribution between lift and plunge velocity, or between pitching moment and pitch rate, the net aerodynamic energy input into the structure over one oscillation cycle decreases. The equivalent aerodynamic damping of the system is then enhanced, which is reflected by a reduction in the flutter-response amplitude.

In terms of operating mode, the pre-wing can be divided into two cases: relatively stationary and actively moving. When the pre-wing remains stationary relative to the main wing, its main function is to modify the mean flow field near the leading edge of the main wing, the wake-interference intensity, and the amplitude distribution of the unsteady aerodynamic forces through its fixed geometric position and size. This mode is similar to a passive aerodynamic interference component and does not require additional control input. It is therefore suitable for analyzing the basic influence of pre-wing position and size on the flutter response. When the pre-wing actively oscillates with a prescribed frequency and amplitude, its wake disturbance has a clear periodic characteristic and may further change the phase relationship between the unsteady aerodynamic forces and the structural motion of the main wing, thereby enabling more direct aerodynamic-energy regulation.

Therefore, this study first investigates the influence of a relatively stationary pre-wing on the free aeroelastic response of the main wing, in order to clarify the effects of pre-wing position and size on structural response amplitude, aerodynamic work, and channel-wise energy distribution. On this basis, active motion parameters of the pre-wing can be further introduced in future work. By controlling the oscillation frequency, amplitude, and phase of the pre-wing, the unsteady aerodynamic characteristics of the main wing may be regulated, providing a basis for active flutter suppression.

To systematically investigate the influence of the pre-wing on the flutter response of the main wing, the combined configuration needs to be parameterized. The size parameters of the pre-wing mainly include its major-axis length and minor-axis length. The major-axis length primarily determines the streamwise geometric scale of the pre-wing and its influence range on the leading-edge flow of the main wing, while the minor-axis ratio affects the thickness of the pre-wing, its flow-circulation characteristics, and wake-disturbance intensity. Therefore, the size parameters directly affect the capability of the pre-wing to modulate the unsteady aerodynamic forces of the main wing.

The position parameters of the pre-wing are determined by the location of its center relative to the leading edge of the main wing. These parameters determine the intensity and acting region of the pre-wing wake, induced velocity, and local flow disturbance when they reach the leading edge of the main wing, and are therefore important factors affecting the plunge–pitch aeroelastic response of the main wing. In addition to size and position parameters, the pre-wing may also have an initial installation angle and active motion parameters. The active motion parameters of the pre-wing affect the temporal characteristics of its wake disturbance, and may therefore further regulate the phase relationship between the unsteady aerodynamic forces and structural motion of the main wing.

Table 1 – Design parameters of the pre-main wing composite configuration

Parameter type	Design parameters	Sign	Nondimensional parameter
Size parameters	Long axis length of the pre-wing	e	$\bar{e} = e / c$
	Short axis length of the pre-wing	d	$\bar{d} = d / e$
Position parameters	Horizontal distance between the center of the pre-wing and the leading edge of the main wing	L_H	$\bar{L}_H = L_H / c$
	Vertical distance between the center of the pre-wing and the leading edge of the main wing	L_V	$\bar{L}_V = L_V / c$

https://doi.org/10.71945/icas2026_0494

	Initial attack angle of the pre-wing	$\alpha_{0,\mathrm{pre}}$	

3. Establishment of the flutter analysis procedure

To obtain the free aeroelastic response of the prepositive elliptical wing–main wing combined configuration under low-speed classical flutter conditions, a numerical analysis procedure based on time-domain computational fluid dynamics (CFD) is established. In this procedure, a baseline computational model is first developed for the single main-wing configuration. A user-defined function (UDF) is used to realize the two-degree-of-freedom free oscillation of the main wing in plunge and pitch, and the near-critical response without the pre-wing is obtained. Then, the prepositive elliptical wing is introduced under the same structural parameters and freestream conditions. The overset-grid method is adopted to handle the relative arrangement and overall motion of the pre-wing and the main wing. By comparing the response amplitudes, aerodynamic work, and aerodynamic-force–structural-motion relationship between the single main wing and the combined configuration, the influence of the pre-wing on the flutter response of the main wing is evaluated.

3.1 Introduction to the overset-grid method

The prepositive elliptical wing–main wing combined configuration consists of two independent aerodynamic components. In subsequent active-control studies, the pre-wing may also move independently relative to the main wing. To conveniently handle multi-body configurations, relative position variations, and moving-boundary problems, the overset-grid method is adopted to establish the computational model. In the overset-grid method, the computational domain is divided into a background grid and several moving sub-grids. Spatial overlap is allowed between different grids, and flow-field information is transferred through interpolation. Compared with the conventional single-domain dynamic-mesh method, the overset-grid method is more suitable for handling relative motion of multiple bodies, independent local-grid updating, and parametric variations of complex configurations.

In the present simulations (Fig 3), the background grid is used to describe the far-field flow region, while the main wing and the pre-wing are each assigned an independent local sub-grid. The main-wing sub-grid moves together with the plunge and pitch motions of the main wing. When the pre-wing remains stationary relative to the main wing, the pre-wing sub-grid and the main wing undergo the same rigid-body motion as a whole. This treatment prevents obvious mesh distortion near the main wing and the pre-wing during motion and also facilitates rapid replacement of local grids for batch calculations under different pre-wing positions and size parameters.

For the baseline single main-wing configuration, the computational domain consists of the background grid and the local grid around the main wing. For the pre-wing–main wing combined configuration, an additional local grid around the pre-wing is introduced based on the single main-wing model. The surfaces of both the main wing and the pre-wing are set as no-slip walls. A velocity-inlet boundary condition is applied at the inlet of the background domain, a pressure-outlet boundary condition is applied at the outlet, and symmetry boundary conditions are applied to the upper and lower boundaries. To ensure the accuracy of unsteady aerodynamic-force calculations, local mesh refinement is applied around both the main wing and the pre-wing, with particular attention paid to the pre-wing wake region and the leading-edge region of the main wing.

https://doi.org/10.71945/icas2026_0494

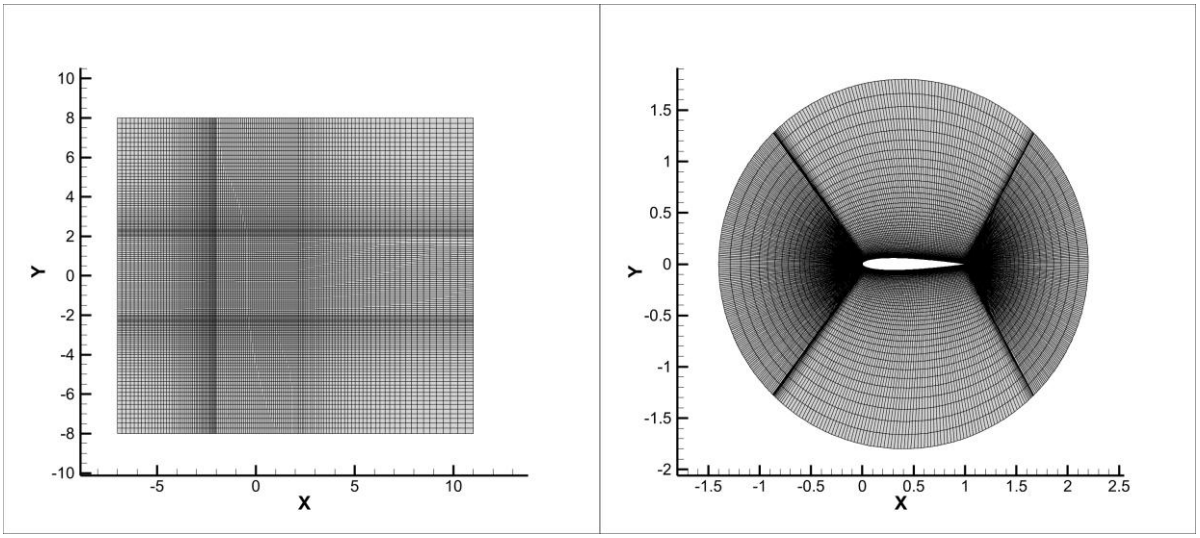


Figure 3 – Farfield background mesh and main wing mesh

The flow field is solved using the incompressible unsteady Reynolds-averaged Navier–Stokes equations. The $k-\omega$ SST turbulence model is adopted. The governing equations are spatially discretized using a second-order upwind scheme, and time advancement is performed using a second-order implicit scheme. This setup can maintain numerical stability while capturing the variation of unsteady aerodynamic forces near the leading edge of the main wing. Within each physical time step, after the flow-field equations converge, the lift-direction aerodynamic force acting on the main wing and the pitching moment about the elastic axis are extracted and transferred to the two-degree-of-freedom structural dynamic equation to update the motion state of the main wing in the next time step.

3.2 Two-degree-of-freedom aeroelastic model

The main wing is simplified as a two-dimensional airfoil section with two degrees of freedom: plunge and pitch. In this two-dimensional airfoil model, inertial coupling exists between the plunge and pitch degrees of freedom. Therefore, the structural mass matrix can be expressed as

$$\mathbf{M}_s = \begin{bmatrix} m & S_\alpha \\ S_\alpha & I_\alpha \end{bmatrix} \tag{6}$$

where m is the equivalent mass per unit span, I_α is the moment of inertia about the elastic axis, and S_α is the static moment. The structural stiffness matrix can be written as

$$\mathbf{K}_s = \begin{bmatrix} K_h & 0 \\ 0 & K_\alpha \end{bmatrix} \tag{7}$$

where K_h is the plunge stiffness and K_α is the pitch stiffness. To more clearly observe the near-critical aeroelastic response, structural damping is not introduced in the baseline calculation. That is, both the plunge and pitch structural damping coefficients are set to zero. This makes it easier to identify whether aerodynamic forces input energy into or dissipate energy from the structural system. Fig 4 shows the graph of the aerodynamic calculation parameters in this paper, Table 2 shows the parameters for the aeroelastic calculations.

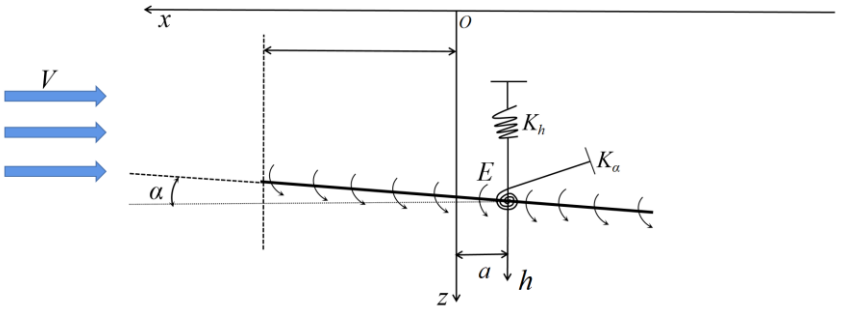


Fig. 4 – Two-degree-of-freedom wing section aeroelastic model

https://doi.org/10.71945/icas2026_0494

Table 2 Aeroelastic parameters of the single main-wing configuration

Parameters	Value
Main wing chord length c	1m
Density ρ	1.225kg/m^3
Freestream velocity V_∞	55m/s
Dimensionless elastic-axis position parameter a	-0.4
Elastic-axis x-coordinate	0.1m
Equivalent plunge mass m_h	19.24kg
Pitch moment of inertia I_α	1.20kg·m²
Static moment S_α	0.65kg·m
Plunge stiffness k_h	4380N/m
Pitch stiffness k_α	350N·m/rad
Plunge structural damping C_h	0
Pitch structural damping C_α	0

In the numerical calculation, a UDF is written to perform the fluid–structure coupling. Within each physical time step, the CFD solver first calculates the lift-direction aerodynamic force $F_y(t)$ and the pitching moment $M_z(t)$ acting on the main wing at the current time. These aerodynamic loads are then substituted into the two-degree-of-freedom structural equation to solve the plunge displacement, pitch angle, and corresponding velocities of the main wing at the next time step. The updated $h(t)$ and $\alpha(t)$ are further used to control the motion of the main-wing grid, thereby realizing time-domain coupling between the flow field and the structural motion.

3.3 Flutter excitation case of the baseline single main-wing configuration

Before analyzing the prepositive elliptical wing–main wing combined configuration, it is necessary to establish the baseline response of the single main wing without the pre-wing. In this study, the NACA0012 airfoil is selected as the main-wing model, with a chord length of c =1m. The computational model of the single main wing consists of the background grid and the local grid around the main wing, and the mesh setup has been introduced in Section 3.1.

At the beginning of the calculation, a small initial disturbance is applied to the main wing, causing it to develop a free aeroelastic response under the combined effects of aerodynamic forces, inertial forces, and structural elastic forces. During the calculation, the lift-direction aerodynamic force, pitching moment, plunge displacement, pitch angle, and corresponding velocity terms of the main wing are recorded as functions of time. By observing whether the response grows, decays, or remains approximately constant in amplitude, it can be determined whether the system is close to the flutter boundary under the current freestream velocity.

At $U_\infty = 55\text{m/s}$, the plunge and pitch responses of the single main-wing configuration gradually develop into approximately constant-amplitude oscillations. This result indicates that the present condition can be used as a baseline state for investigating the free aeroelastic response of the main wing near the critical flutter condition. After the prepositive elliptical wing is introduced, if the plunge and pitch amplitudes of the main wing are lower than those of the baseline configuration, or if the net aerodynamic work done on the structural system decreases, the pre-wing can be considered to have a weakening effect on the flutter response of the main wing.

https://doi.org/10.71945/icas2026_0494

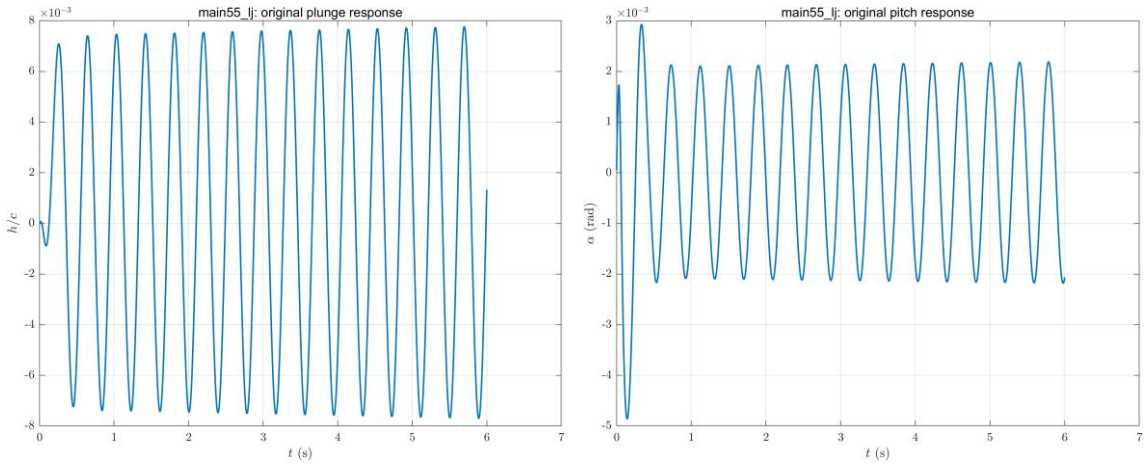


Fig 5 – Free plunge and pitch response curves of the single main-wing configuration

In addition to the structural response, the plunge-channel, pitch-channel, and total aerodynamic work of the single main-wing configuration are extracted as the baseline for the subsequent energy analysis of the combined configuration. For the baseline single main-wing configuration, aerodynamic work reflects the net energy input from the aerodynamic forces into the structural system over one oscillation cycle. After the pre-wing is introduced, comparing the channel-wise aerodynamic work under the same freestream velocity and structural parameters can further determine whether the pre-wing changes the aerodynamic energy-input path of the main wing.

In summary, this section establishes the computational procedure for the free aeroelastic response of the single main-wing configuration and obtains an approximately constant-amplitude oscillatory response near the critical condition at $U_\infty = 55\mathrm{m/s}$. This result provides a unified baseline for the subsequent parametric calculations of the prepositive elliptical wing–main wing combined configuration and serves as a reference for evaluating whether the pre-wing reduces the structural response amplitude and aerodynamic energy input.

4. Simulations of the prepositive elliptical wing–main wing combined configuration

To investigate the influence of the prepositive elliptical wing on the low-speed classical flutter response of the main wing, a numerical simulation model of the prepositive elliptical wing–main wing combined configuration is further established based on the two-degree-of-freedom free aeroelastic response calculation of the single main wing. At the present stage, the pre-wing is mainly considered to be stationary relative to the main wing. In other words, the pre-wing is arranged near the leading edge of the main wing as a fixed aerodynamic interference component and undergoes the same overall plunge–pitch free oscillation as the main wing. By varying the nondimensional horizontal and vertical distances between the pre-wing center and the leading edge of the main wing, the aeroelastic responses of the combined configuration under different position parameters are analyzed and compared with those of the baseline single main-wing configuration.

Based on the previous studies of the research group on the flow-control characteristics of this combined configuration[20], representative pre-wing size parameters that show favorable aerodynamic performance under both static-stall and dynamic-stall conditions are adopted in this study, so as to maintain the original flow-control capability as much as possible. In the position-parameter study, the nondimensional major-axis length of the prepositive elliptical wing is set to $\bar{e}$ =0.025, the nondimensional minor-axis length is set to $\bar{d}$ =0.15, and the initial installation angle is set to $\alpha_{0,\mathrm{pre}}$ =-1° . Subsequently, near the favorable positions identified from the position-parameter analysis, the major-axis length of the pre-wing is further varied to analyze the influence of size variation on the flutter response.

4.1 Evaluation method for the flutter suppression effect of the prepositive elliptical wing

To evaluate the influence of the pre-wing on the flutter response of the main wing, this study analyzes the results from three aspects: structural response amplitude, aerodynamic work, and the time evolution of aerodynamic forces and structural velocities.

First, the dynamic amplitudes of plunge and pitch are used to evaluate the structural response intensity of the main wing. For each computational case, several relatively stable cycles in the later

https://doi.org/10.71945/icas2026_0494

stage of the simulation are selected, and the maximum and minimum values of plunge displacement and pitch angle are extracted. The dynamic amplitudes of plunge and pitch are defined as

$$A_h = \frac{h_{\max} - h_{\min}}{2}, \quad A_\alpha = \frac{\alpha_{\max} - \alpha_{\min}}{2} \tag{8}$$

To evaluate the response variation of the combined configuration relative to the single main-wing configuration, the plunge-amplitude reduction ratio and pitch-amplitude reduction ratio are further defined as

$$\eta_h = \frac{(A_h)_{\text{base}} - (A_h)_{\text{pre}}}{(A_h)_{\text{base}}} \times 100\%, \quad \eta_\alpha = \frac{(A_\alpha)_{\text{base}} - (A_\alpha)_{\text{pre}}}{(A_\alpha)_{\text{base}}} \times 100\% \tag{9}$$

where the base denotes the baseline single main-wing configuration, and the pre denotes the pre-wing–main wing combined configuration. When $\eta_h > 0$ or $\eta_\alpha > 0$, the pre-wing reduces the response amplitude of the corresponding degree of freedom. When the value is negative, the pre-wing instead enhances the vibration response of the corresponding degree of freedom at that position.

Second, aerodynamic work is used to evaluate the influence of the pre-wing on the aerodynamic energy input of the system. For a two-degree-of-freedom aeroelastic system, the aerodynamic work done on the structure can be decomposed into the plunge and pitch channels. In this study, the periods of the plunge and pitch responses are identified separately, and the final N cycles in the later stage of the simulation are selected for integration, where N =3. The cycle-averaged aerodynamic work of the plunge and pitch channels is defined as

$$\begin{cases} W_h &= \dfrac{1}{NT_h} \displaystyle\int_{t_{h,0}}^{t_{h,0}+NT_h} F_y(t)\dot{h}(t)dt \\ W_\alpha &= \dfrac{1}{NT_\alpha} \displaystyle\int_{t_{\alpha,0}}^{t_{\alpha,0}+NT_\alpha} M_z(t)\dot{\alpha}(t)dt \end{cases} \tag{10}$$

where $F_y(t)$ is the lift-direction aerodynamic force acting on the main wing, $M_z(t)$ is the pitching moment about the elastic axis, and $\dot{h}$ and $\dot{\alpha}$ are the plunge velocity and pitch rate, respectively. To facilitate comparison among different configurations, the nondimensional aerodynamic work is further defined as

$$\begin{cases} C_{W,h} &= \dfrac{W_h}{\frac{1}{2}\rho V_\infty^3 cb} \\ C_{W,\alpha} &= \dfrac{W_\alpha}{\frac{1}{2}\rho V_\infty^3 cb} \end{cases} \tag{11}$$

Aerodynamic work reflects the net energy input from aerodynamic forces to the structural system over one cycle. When the aerodynamic work decreases, the equivalent aerodynamic damping of the system increases, and the structural response is more likely to be suppressed.

Finally, the cycle-normalized time-evolution curves of aerodynamic forces and structural velocities are plotted. For the plunge channel, the variations of the nondimensional lift-direction aerodynamic force C_{F_y} and nondimensional plunge velocity h/c with normalized time are compared. For the pitch channel, the variations of the nondimensional pitching moment C_{M_z} and pitch rate α with normalized time are compared. These curves can directly show whether the aerodynamic-force peaks lead or lag the structural-velocity peaks, and therefore indicate whether the pre-wing changes the phase relationship between aerodynamic forces and structural response.

4.2 Influence of pre-wing position on flutter response

Figure 6 presents the position distributions of the plunge- and pitch-amplitude reduction ratios under different pre-wing positions. It can be seen that the pre-wing placement has a clear influence on the two-degree-of-freedom free aeroelastic response of the main wing. For most combined configurations, both the plunge and pitch response amplitudes are lower than those of the single

https://doi.org/10.71945/icas2026_0494

main-wing configuration. This indicates that, under the present low-speed classical flutter condition, a properly arranged pre-wing can weaken the aeroelastic response of the main wing.

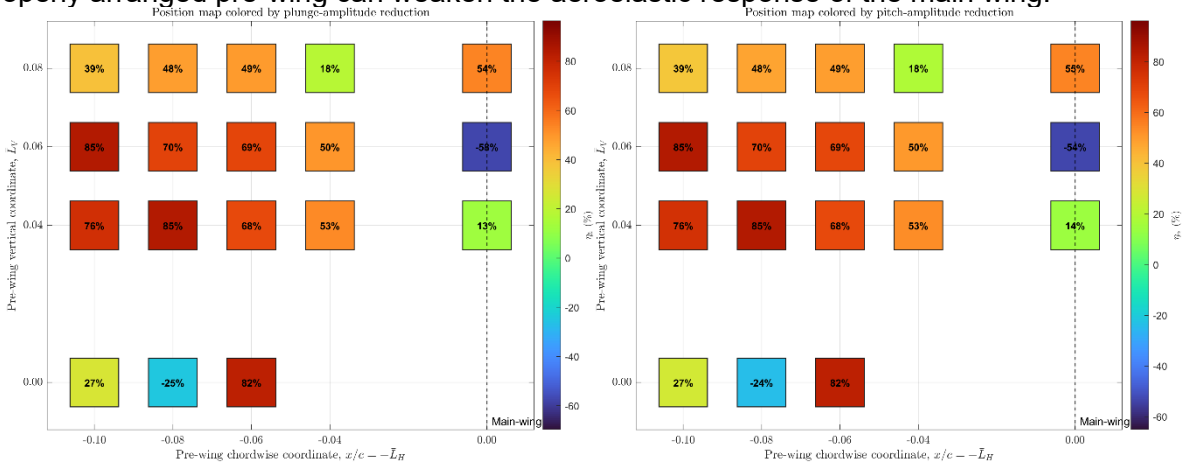


Fig 6 – Distributions of plunge- and pitch-amplitude reduction ratios under different pre-wing positions

From the plunge-amplitude reduction distribution, the relatively favorable region is mainly located around $\bar{L}_H$ =0.08~0.1 and $\bar{L}_V$ =0.04~0.06. In particular, the positions (0.08,0.04) and (0.10,0.06) both achieve a plunge-amplitude reduction of approximately 85%, making them representative configurations with strong suppression in the plunge direction within the present computational range. To facilitate comparison with the displacement of the single main wing, all displacement responses are demeaned. The variation trend of pitch amplitude is basically consistent with that of plunge amplitude, and the pitch-amplitude reduction ratio also reaches approximately 85% at the above two positions. This indicates that the pre-wing at these positions does not merely suppress a single degree of freedom, but weakens the coupled plunge–pitch response as a whole.

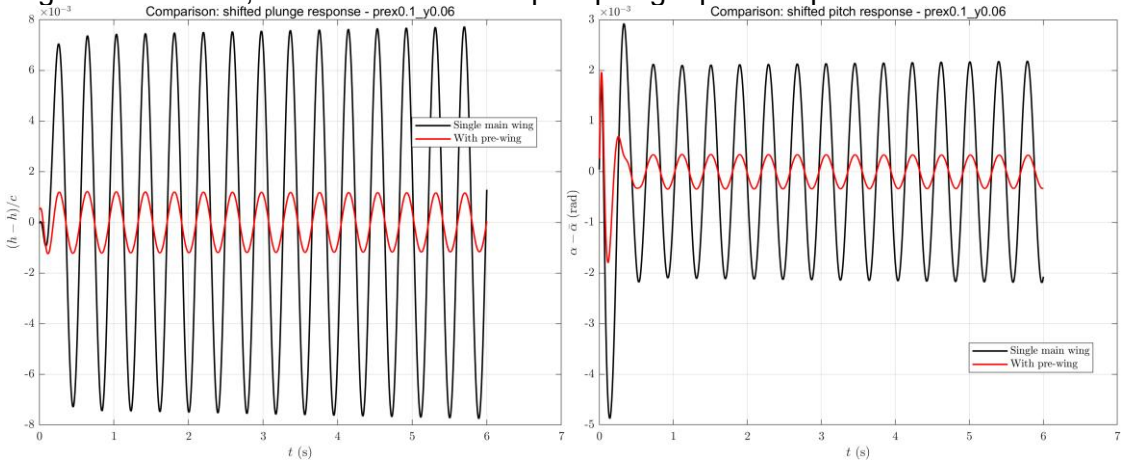


Fig 7 – $(\bar{L}_H, \bar{L}_V) = (0.10, 0.06)$ time-amplitude response

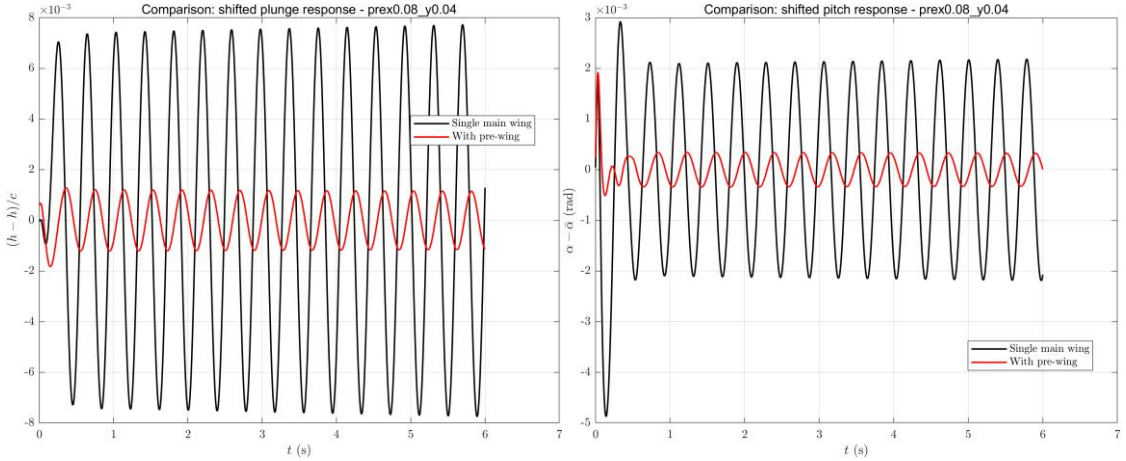


Fig 8 – $(\bar{L}_H, \bar{L}_V) = (0.08, 0.04)$ time-amplitude response

From the position-distribution trend, the amplitude reduction ratio does not vary monotonically with

https://doi.org/10.71945/icas2026_0494

$\bar{L}_H$ and $\bar{L}_V$. When the horizontal distance is too small, the pre-wing produces strong interference with the flow near the leading edge of the main wing, which may enhance local aerodynamic fluctuations. When the horizontal distance is too large, the wake of the pre-wing may decay before reaching the leading edge of the main wing, weakening its modulation effect on the unsteady aerodynamic forces of the main wing. Therefore, a relatively appropriate spatial distance exists between the pre-wing and the main wing. The present results indicate that moderately increasing the horizontal distance between the pre-wing and the leading edge of the main wing, while maintaining a certain vertical spacing, is beneficial for reducing the plunge and pitch response amplitudes of the main wing.

To further explain the variation in response amplitude, the aerodynamic work at different positions is analyzed. Figure 9 presents the reduction ratio of the total nondimensional aerodynamic work under different pre-wing positions, while Figure 10 presents the reduction ratios of the nondimensional aerodynamic work in the plunge and pitch channels. The results of total nondimensional aerodynamic work show that most pre-wing configurations can significantly reduce the total aerodynamic energy input of the system. The total-work reduction ratio is mainly distributed around 98%~113%. This indicates that, for most positions, the introduction of the pre-wing weakens the net energy input from aerodynamic forces to the structural system, which is consistent with the overall trend of reduced structural response amplitudes.



Fig 9 – Distribution of the total nondimensional aerodynamic-work reduction ratio under different pre-wing positions.

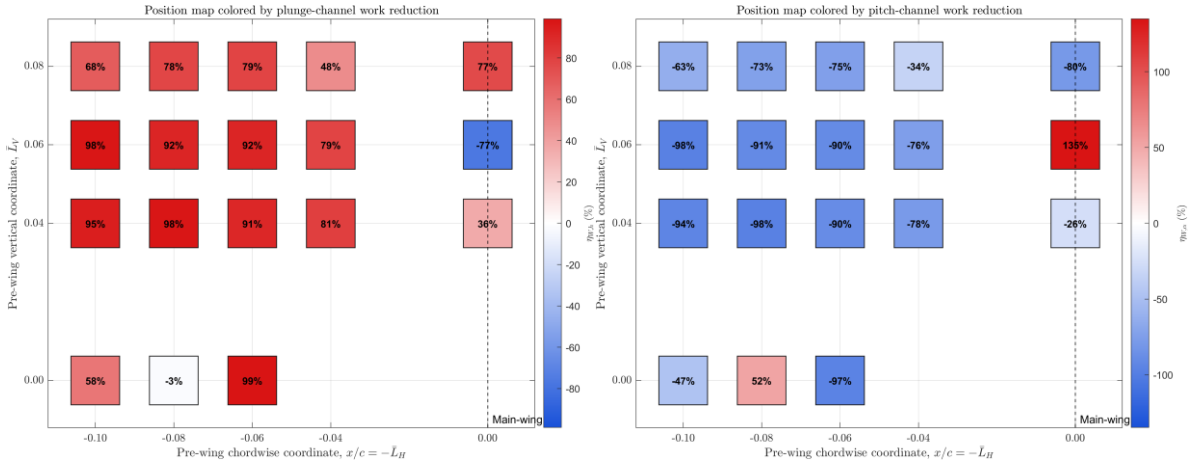


Fig 10 – Distributions of the plunge- and pitch-channel aerodynamic-work reduction ratios under different pre-wing positions

Further analysis of the channel-wise aerodynamic work shows that the plunge channel is the main contributor to the variation in total work for the present configuration. Taking (0.08,0.04) and (0.10,0.06) as examples, the reduction ratios of the plunge-channel work are both close to 98%, indicating that the pre-wing significantly weakens the energy input from lift to the plunge motion. Although the pitch-channel work may increase to some extent at some favorable positions, the large reduction in plunge-channel work dominates. Therefore, the total aerodynamic energy input of the

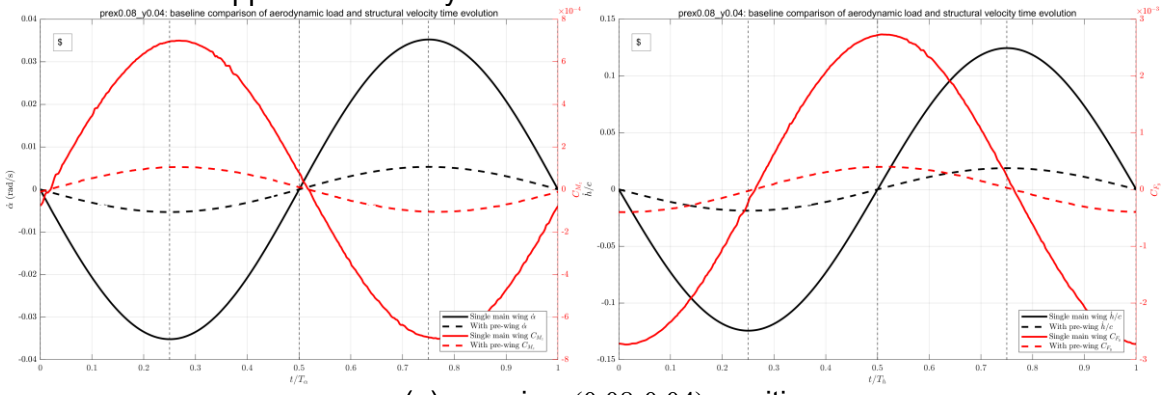
https://doi.org/10.71945/icas2026_0494

system is still significantly reduced, which finally appears as simultaneous reductions in the plunge and pitch response amplitudes.

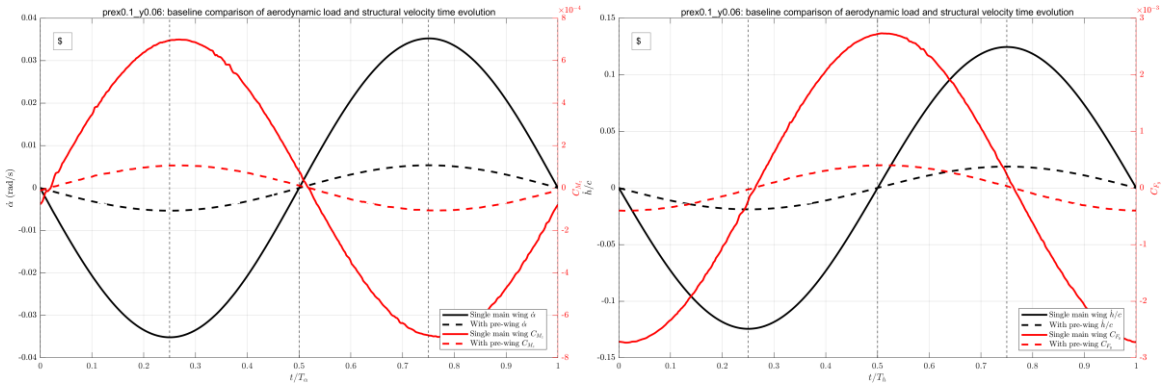
It is worth noting that the two positions (0.08,0) and (0,0.06) show special behavior. Although the reduction ratios of total nondimensional aerodynamic work at these two positions are relatively high, approximately 323% and 303%, respectively, the structural response amplitudes do not decrease but instead increase. The channel-wise work decomposition indicates that this phenomenon is mainly related to the inconsistent energy distribution between the plunge and pitch channels. At these positions, the pre-wing may significantly reduce the pitch-channel aerodynamic work, but its suppression of the plunge channel, which dominates the current response growth, may be insufficient; it may even increase the plunge-channel work. Therefore, although the total work decreases significantly due to cancellation between channels, the structural response amplitude may still increase.

These results demonstrate that the reduction ratio of total aerodynamic work alone cannot fully determine the flutter suppression effect of the pre-wing configuration. For a two-degree-of-freedom aeroelastic system, the aerodynamic energy input in the plunge and pitch channels may follow different trends. If the reduction in one channel masks an increase in energy input in the other channel, the total-work result may not be fully consistent with the response-amplitude variation. Therefore, when evaluating the flutter suppression effect of the pre-wing, the plunge amplitude, pitch amplitude, plunge-channel work, pitch-channel work, and total work should be considered together.

Figure 11 shows the cycle-normalized time evolution of aerodynamic forces and structural velocities for representative favorable and special configurations. For the favorable configurations (0.08,0.04) and (0.10,0.06), after the pre-wing is introduced, the correspondence between lift and plunge velocity changes in a favorable manner, reducing the positive-work contribution in the plunge channel. As a result, the plunge-channel aerodynamic work is significantly reduced. For the special configurations (0.08,0) and (0,0.06), although the pre-wing weakens part of the pitching-moment work, a strong positive-work region still exists between lift and plunge velocity, making the plunge response difficult to suppress effectively.

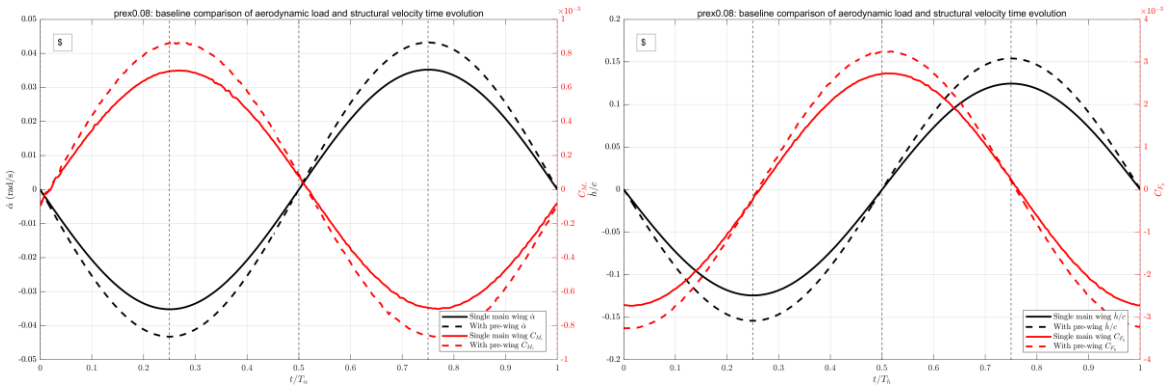


(a) pre-wing $(0.08, 0.04)$ position

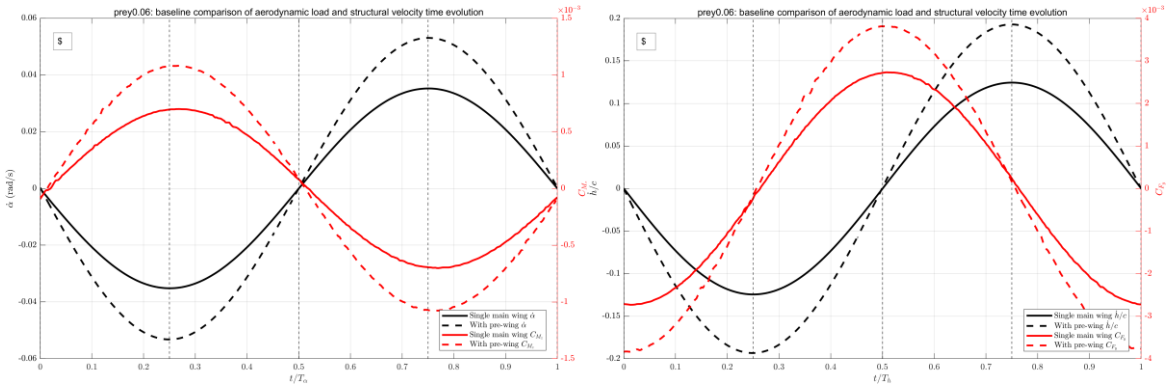


(b) pre-wing $(0.10, 0.06)$ position

https://doi.org/10.71945/icas2026_0494



(c) pre-wing $(0.08, 0)$ position



(d) pre-wing $(0, 0.06)$ position

Fig 11 – Cycle-normalized time evolution of aerodynamic forces and structural velocities for representative configurations

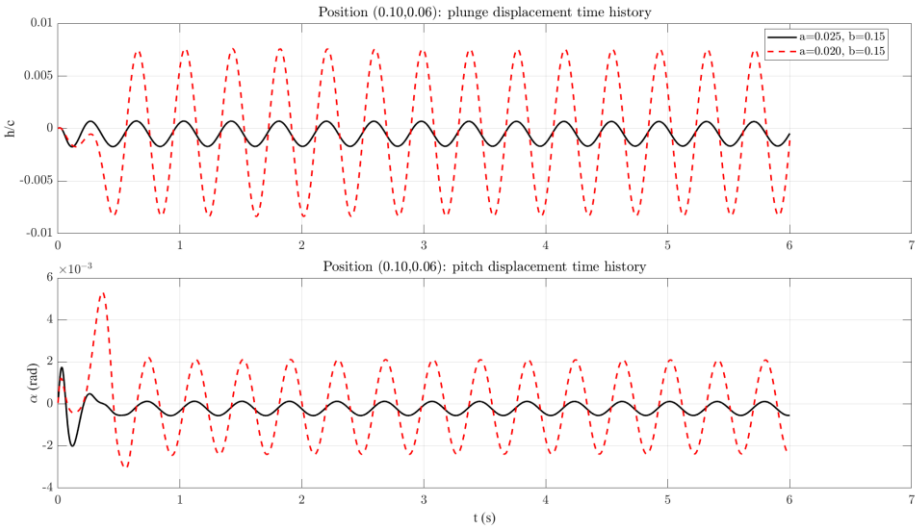
It can also be observed from the figure that the relatively stationary pre-wing does not significantly influence the dominant phase relationship between aerodynamic forces and structural velocities. For both favorable and special configurations, the main peak positions and zero-crossing locations of aerodynamic forces and structural velocities do not change significantly. This indicates that, under the present fixed pre-wing condition, the influence of the pre-wing on the flutter response is mainly reflected in the variation of aerodynamic-force amplitudes and the redistribution of energy between the plunge and pitch channels, rather than in a significant change in the phase relationship between aerodynamic forces and structural motion. If the flutter suppression effect is to be further enhanced through phase regulation, the active motion law of the pre-wing relative to the main wing should be considered in future work.

4.3 Influence of pre-wing size on flutter response

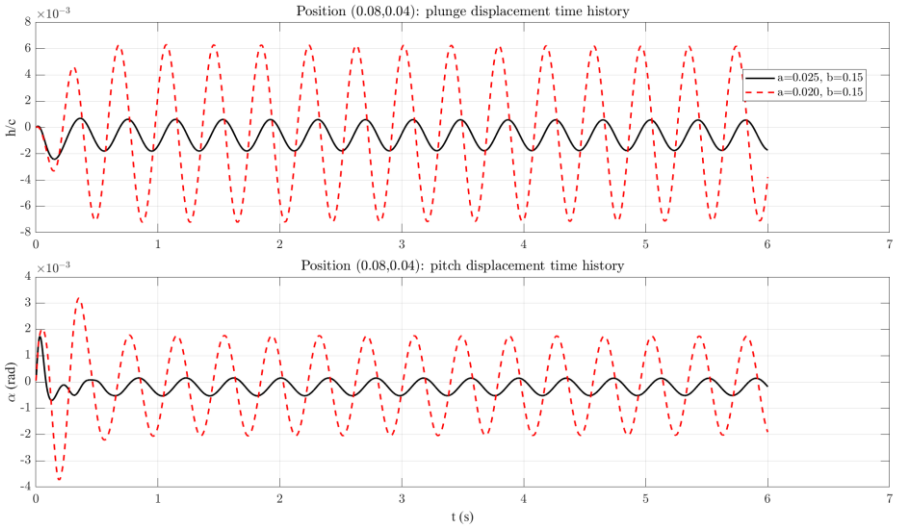
After completing the position-parameter analysis, this study further investigates the influence of pre-wing size parameters at selected favorable positions. Since the major-axis length of the pre-wing directly affects its streamwise geometric scale, wake strength, and interference range on the leading-edge flow of the main wing, the major-axis length is varied first while the minor-axis ratio is kept unchanged, at 0.15. The aeroelastic responses of the combined configuration under different major-axis lengths are then compared.

Based on the position-parameter analysis in the previous section, several favorable positions are selected to compare the variations in plunge amplitude, pitch amplitude, and aerodynamic work under different major-axis lengths. First, the minor-axis ratio of the pre-wing is kept constant at $\bar{d} = 0.15$, while $\bar{e} = 0.025$ and $\bar{e} = 0.02$ are selected to investigate the influence of size variation on the flutter response of the main wing. The results show that when the major-axis length of the pre-wing is reduced, the vibration amplitudes at these favorable positions increase.

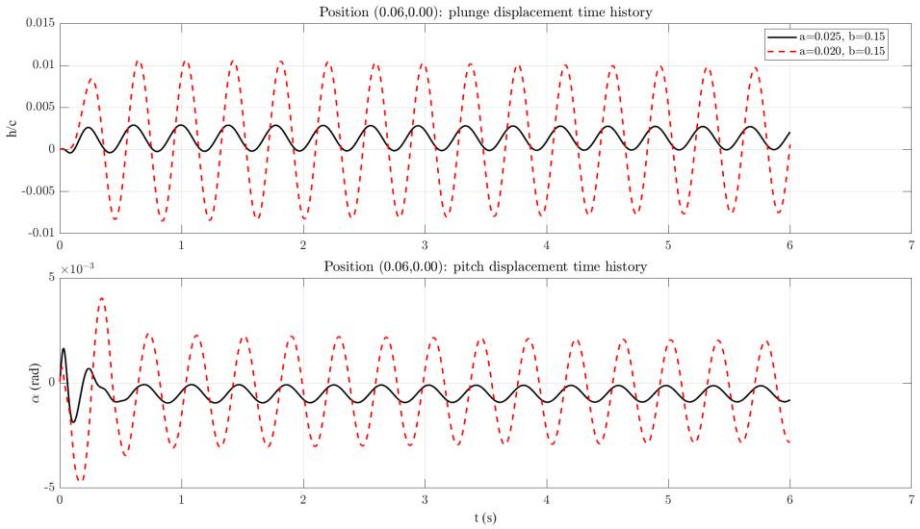
https://doi.org/10.71945/icas2026_0494



(a)



(b)



(c)

Fig 11 – Comparison of response amplitudes under different pre-wing sizes at favorable positions

As shown in Fig 11, the variation in the major-axis length of the pre-wing clearly affects the flutter suppression effect of the combined configuration. When the major-axis length is reduced from $\overline{e} = 0.025$ to $\overline{e} = 0.02$, the plunge and pitch response amplitudes increase at some favorable positions. This indicates that, under the present freestream condition and structural parameters, an excessively small pre-wing major-axis length may be insufficient to provide adequate modulation of the unsteady flow near the leading edge of the main wing, thereby weakening the flutter

https://doi.org/10.71945/icas2026_0494

suppression effect originally obtained at these positions.

From the physical-mechanism perspective, the pre-wing needs to influence the incoming-flow condition near the leading edge of the main wing through its own flow circulation and wake. When the major-axis length is relatively small, the disturbance range and wake strength of the pre-wing are weakened, and its ability to regulate the lift and pitching moment of the main wing decreases. Consequently, its ability to reduce aerodynamic energy input also weakens. Conversely, a moderate increase in the major-axis length of the pre-wing can enhance its influence on the leading-edge flow of the main wing. However, if the size is too large, it may lead to excessively strong local interference and even large aerodynamic-force fluctuations. Therefore, the major-axis length of the pre-wing should be selected by balancing sufficient aerodynamic modulation capability with the avoidance of excessive local disturbance.

The present size-parameter results indicate that the major-axis length of the pre-wing is an important geometric parameter affecting the flutter suppression effect of the combined configuration. Among the representative cases completed in this study, the configuration with ($\bar{a}=0.025$) and ($\bar{b}=0.15$) shows relatively favorable overall performance and can reduce both plunge and pitch response amplitudes at several favorable positions. It should be noted that the present size analysis is still a preliminary parametric comparison. A more systematic scan over a wider size range is still required in future work to further clarify the relationship between pre-wing size and flutter response.

4.4 Summary of observed trends

Based on the completed position- and size-parameter calculations, the following preliminary trends can be obtained.

First, the prepositive elliptical wing clearly influences the two-degree-of-freedom free aeroelastic response of the main wing. At most positions, after the pre-wing is introduced, the plunge and pitch amplitudes of the main wing are lower than those of the single main-wing configuration. This indicates that the combined configuration has the potential to weaken the structural response under low-speed classical flutter conditions.

Second, the pre-wing position has a significant influence on the flutter suppression effect. The relatively favorable region is mainly located around ($\bar{L}_H=0.08\sim0.10$) and ($\bar{L}_V=0.04\sim0.06$). Positions such as ((0.08,0.04)) and ((0.10,0.06)) can reduce both plunge and pitch response amplitudes and significantly decrease the aerodynamic work in the plunge channel. These positions are therefore relatively favorable pre-wing placements within the present computational range.

Third, the reduction in plunge-channel work is an important reason for the decrease in response amplitude of the present configuration. For favorable configurations, the pre-wing mainly reduces the energy input from lift to the plunge motion, thereby decreasing the total aerodynamic energy input of the system and weakening the coupled plunge–pitch response. In contrast, at some special positions, although the total aerodynamic-work reduction ratio is relatively high, the structural response amplitude may still increase because of the uncoordinated energy distribution between the plunge and pitch channels. Therefore, the evaluation of the pre-wing configuration should not rely only on total work, but should combine channel-wise work and response amplitude.

In addition, the relatively stationary pre-wing does not significantly change the dominant phase relationship between aerodynamic forces and structural velocities. The fixed pre-wing mainly affects the flutter response by changing the aerodynamic-force amplitude and the energy distribution between the plunge and pitch channels, rather than by significantly changing the aerodynamic-force phase. This result indicates that, if the flutter suppression effect is to be further enhanced using phase regulation, active pre-wing motion parameters should be investigated in future work.

5. Conclusions

This paper investigates the flutter characteristics of a two-dimensional prepositive elliptical wing–main wing combined configuration under low-speed classical flutter conditions. A time-domain CFD-based aeroelastic analysis method is established. The main wing is modeled as a NACA0012 airfoil with plunge and pitch degrees of freedom, and the structural motion is coupled with the unsteady aerodynamic loads through a user-defined function. An overset-grid method is adopted to construct the pre-wing–main wing combined configuration and to facilitate the position and size variation of the pre-wing. Based on the numerical results, the following conclusions can be drawn.

https://doi.org/10.71945/icas2026_0494

First, the established numerical method can capture the free aeroelastic response of the single main-wing baseline configuration. Under the selected condition of $U_\infty = 55\mathrm{m/s}$, the baseline main wing develops a nearly constant-amplitude plunge–pitch response. This result provides a reference case for evaluating the influence of the prepositive elliptical wing on the aeroelastic response.

Second, the prepositive elliptical wing has a clear influence on the two-degree-of-freedom aeroelastic response of the main wing. For most of the investigated positions, the plunge and pitch amplitudes of the combined configuration are lower than those of the single main wing. This indicates that a properly arranged pre-wing can weaken the aeroelastic response of the main wing under the present low-speed classical flutter condition.

Third, the suppression effect is strongly dependent on the pre-wing position. Within the investigated design space, relatively favorable regions are mainly located around $\bar{L}_H = 0.08 \sim 0.10$ and $\bar{L}_V = 0.04 \sim 0.06$. In particular, the positions $(\bar{L}_H, \bar{L}_V) = (0.08, 0.04)$ and $(0.1, 0.06)$ show significant reductions in both plunge and pitch amplitudes, with the maximum amplitude reduction reaching approximately 85%. These results suggest that the horizontal and vertical distances between the pre-wing and the main-wing leading edge should be considered simultaneously, rather than optimized independently.

Fourth, the aerodynamic-work analysis shows that the reduction in the plunge-channel work is the main contributor to the suppressed response. For the favorable positions, the plunge-channel aerodynamic work is reduced by approximately 98%, which is consistent with the significant reduction in structural response amplitudes. However, the total aerodynamic work is not always sufficient to evaluate the suppression effect. At some special positions, such as (0.08,0) and (0,0.06), the total nondimensional aerodynamic work decreases significantly, but the structural response amplitude still increases. This is caused by the inconsistent energy contributions of the plunge and pitch channels. Therefore, the evaluation of the pre-wing effect should combine response amplitudes, total aerodynamic work, and channel-wise aerodynamic work.

Fifth, the time-evolution analysis of aerodynamic forces and structural velocities indicates that the relatively stationary pre-wing does not significantly change the dominant phase relationship between the aerodynamic loads and the structural velocities. Its influence is mainly reflected in the modification of aerodynamic-force amplitudes and the redistribution of aerodynamic energy between the plunge and pitch channels. This implies that, for a stationary pre-wing, flutter-response reduction is achieved mainly through amplitude and energy redistribution rather than strong phase control.

Finally, the preliminary size study shows that the major-axis length of the pre-wing is an important geometric parameter. When the major-axis length is reduced while the minor-axis ratio remains unchanged, the response amplitudes at several favorable positions increase. This indicates that an excessively small pre-wing may not provide sufficient flow interference to effectively modify the unsteady aerodynamic loads on the main wing. Therefore, the pre-wing size should be selected by balancing sufficient aerodynamic interference and the avoidance of excessive local flow disturbance.

The present study is still a preliminary two-dimensional numerical investigation. The pre-wing is mainly considered to be stationary relative to the main wing, and the effects of active pre-wing motion, wider design-space exploration have not yet been fully investigated. Future work will focus on the influence of pre-wing motion amplitude, frequency, and phase, as well as three-dimensional aeroelastic simulations, to further clarify the active flutter-control potential of the combined configuration.

6. Contact Author Email Address

Congyu Zhao:zhaocy432@163.com

7. Copyright Statement

The authors confirm that they, and/or their company or organization, hold copyright on all of the original material included in this paper. The authors also confirm that they have obtained permission, from the copyright holder of any third party material included in this paper, to publish it as part of their paper. The authors confirm that they give permission, or have obtained permission from the copyright holder of this paper, for the publication and distribution of this paper as part of the ICAS proceedings or as individual off-prints from the proceedings.

https://doi.org/10.71945/icas2026_0494

References

[1] Theodorsen T. General theory of aerodynamic instability and the mechanism of flutter. NACA Report No. 496, 1935.

[2] Bisplinghoff R L, Ashley H and Halfman R L. *Aeroelasticity*. Addison-Wesley, 1955.

[3] Kratochvíl A and Valenta J. Active flutter suppression for light sport aircraft by a control surface split. *CEAS Aeronautical Journal*, Vol. 15, pp 977–998, 2024.

[4] Wagner H. Über die Entstehung des dynamischen Auftriebes von Tragflügeln. *Zeitschrift für Angewandte Mathematik und Mechanik*, Vol. 5, pp 17–35, 1925.

[5] Petot D. Differential equation modeling of dynamic stall. *La Recherche Aérospatiale*, No. 5, pp 59–71, 1989.

[6] Leishman J G and Beddoes T S. A semi-empirical model for dynamic stall. *Journal of the American Helicopter Society*, Vol. 34, No. 3, pp 3–17, 1989.

[7] Goman M and Khrabrov A. State-space representation of aerodynamic characteristics of an aircraft at high angles of attack. *Journal of Aircraft*, Vol. 31, No. 5, pp 1109–1115, 1994.

[8] Tang D and Dowell E H. Experimental aeroelastic models design and wind tunnel testing for correlation with new theory. *Aerospace*, Vol. 3, No. 2, Article 12, 2016.

[9] Skujins T and Cesnik C E S. Reduced-order modeling of unsteady aerodynamics across multiple Mach regimes. *Journal of Aircraft*, Vol. 51, No. 6, pp 1681–1704, 2014.

[10] Nissim E. Flutter suppression using active controls based on the concept of aerodynamic energy. NASA TN D-6199, 1971.

[11] Behal A, Marzocca P, Rao V M and Gnann A. Nonlinear adaptive control of an aeroelastic two-dimensional lifting surface. *Journal of Guidance, Control, and Dynamics*, Vol. 29, No. 2, pp 382–390, 2006.

[12] Na S, Librescu L, Marzocca P and Kim D. Aeroelastic response of flapped wing systems using robust estimation methodology. *Proceedings of the 45th AIAA/ASME/ASCE/AHS/ASC Structures, Structural Dynamics and Materials Conference*, 2004.

[13] Yu M L, Wen H and Hu H Y. H_∞control for flutter suppression of a two-dimensional airfoil section. *Journal of Vibration Engineering*, Vol. 19, No. 3, pp 326–330, 2006. [in Chinese]

[14] Yu M L, Wen H and Hu H Y. μcontrol for flutter suppression of a two-dimensional airfoil section. *Acta Aeronautica et Astronautica Sinica*, Vol. 28, No. 2, pp 340–343, 2007. [in Chinese]

[15] Hou Y Z, Wang Q and Li G. Robust adaptive switching control for wing flutter. *Acta Aeronautica et Astronautica Sinica*, Vol. 31, No. 2, pp 327–334, 2010. [in Chinese]

[16] Si Y P and Zhao Y H. Wing flutter suppression based on LQG self-tuning regulator. *Journal of Dynamics and Control*, Vol. 10, No. 2, pp 177–181, 2012. [in Chinese]

[17] Han J H, Tani J and Qiu J. Active flutter suppression of a lifting surface using piezoelectric actuation and modern control theory. *Journal of Sound and Vibration*, Vol. 291, No. 3–5, pp 706–722, 2006.

[18] Chen Z, Shi Z, Chen S and Yao Z. Stall flutter suppression of NACA 0012 airfoil based on steady blowing. *Journal of Fluids and Structures*, Vol. 109, Article 103472, 2022.

[19] Mi B and Bai X. New flow control techniques with prepositioned stationary or vibrating elliptical wing at low speed and high angle of attack. *Journal of Aerospace Engineering*, Vol. 35, No. 5, Article 04022064, 2022.

[20] Bai X, Zhan H and Mi B. Unsteady aerodynamic force modeling method for prepositive elliptical wing-main wing composite flow control configurations at high angles of attack. *Physics of Fluids*, Vol. 37, Article 065140, 2025.